

Comparison and Verification of The Results of The GTN Damage Model and The Porous Metal Plasticity Model in The Square Deep Drawing Process

Navid Givianpour¹

Department of Mechanical Engineering,
Aligoudarz Branch, Islamic Azad University,
Aligoudarz, Iran
E-mail: Navidgivianpour@gmail.com

Hamed Deilami Azodi^{2,*}

Department of Mechanical Engineering,
Arak University of Technology, Arak, Iran
E-mail: hamed.azodi@gmail.com
*Corresponding author

Shahrouz Yousefzadeh³

Department of Mechanical Engineering,
Aligoudarz Branch, Islamic Azad University, Aligoudarz, Iran
E-mail: sh.yousefzadeh@yahoo.com

Siamak Mazdak⁴

Engineering faculty, Tafresh University, Tafresh, Iran
E-mail: si.mazdak@tafreshu.ac.ir

Received: 19 August 2024, Revised: 15 January 2025, Accepted: 18 February 2025

Abstract: One of the main goals in the deep drawing process is to achieve a greater drawing depth without causing damage to the sheet; therefore, the drawing ratio is critical in this process. Maximizing the drawing depth has always been the goal of many studies. In this paper, the square deep drawing process is modeled in ABAQUS/Standard finite element software, and then the process is analyzed using the GTN damage model that is implemented by writing a UMAT subroutine. The process is also analyzed based on the porous metal plasticity model available in ABAQUS. The results obtained from these two analyses are compared, providing a comprehensive understanding of the different approaches in deep drawing process analysis. By examining the results, it was found that the results obtained using the GTN damage model are more consistent with the results obtained using the experimental method than the porous metal plasticity model.

Keywords: ABAQUS, Deep Drawing, Drawing Depth, GTN Damage Model, Porous Metal Plasticity

Biographical notes: **Navid Givianpour** received his MSc from Aligoudarz Branch, Islamic Azad University in 2008. His research interests include metal forming and machining. **Hamed Deilami Azodi** received his Ph.D. in Mechanical Engineering from Tarbiat Modarres University, Tehran, Iran in 2008. His research interests include metal forming and advanced mechanical systems. **Shahrouz Yousefzadeh** received his Ph.D. in Mechanical Engineering from the Science and Research Branch of Islamic Azad University in 2011. His research interests focus on computational and applied mechanics. **Siamak Mazdak** received his Ph.D. in Mechanical Engineering from Tarbiat Modares University in 2013. His research interests include the finite element method, metal forming, and numerical analysis.

Research paper

COPYRIGHTS

© 2025 by the authors. Licensee Islamic Azad University Isfahan Branch. This article is an open access article distributed under the terms and conditions of the Creative Commons Attribution 4.0 International (CC BY 4.0)

<https://creativecommons.org/licenses/by/4.0/>



1 INTRODUCTION

The deep drawing process is widely used among metal forming processes because it can create different geometries. In this process, the sheet is formed in the space between the punch and the die by applying force. Regarding the sheet's fracture, the drawing depth in this process is crucial because the strain is usually a tensile strain [1-2].

In general, the deep drawing process involves parameters such as the blank holder force, clearance between punch and die, surface conditions of sheet and tools, geometry of die, and corner radius of punch and die that affect the maximum drawing depth. The effect of each parameter can be investigated using experimental tests or numerical analyses.

Usually, defects such as wrinkling, earing, and rupture may occur in this process, which can be fixed to a large extent by modifying the parameters affecting the process [3]. The deep drawing process is widely used in forming parts in the automotive industry. Since one of the goals in the automotive industry is to reduce weight along with the necessary strength of the car body, alloys with this feature are usually considered. However, these sheets may be prone to failure due to their anisotropic properties. It is necessary to evaluate their behavior with damage models to predict the sheet behavior [4]. In the metal forming processes, various factors affect the successful forming of the sheet, one of the most important of which is the sheet's formability. Usually, in deep drawing, the main goal is to increase the drawing depth, so to optimize this parameter, it can be simulated and numerically analyzed with existing damage models. Chen and Lin [5] studied the square deep drawing process and its effective parameters experimentally and numerically. In a study by Padmanabhan et al. [6], the effect of friction coefficient, blank holder force, and punch radius in the deep drawing process was investigated.

The Gurson damage model [7], a significant development in the field, is one of the various damage models used for the numerical analysis of sheet behavior in metal forming processes. According to Gurson's point of view, the evolution of the voids leads to a decrease in the load-bearing capacity (force) and, finally, the ductile failure of the material. In this model, the nucleation of the new voids during the application of strain is not considered. In other words, only the growth of pre-existing voids is considered.

Tvergaard and Needleman [8-10] proposed a model based on the Gurson model, in which the nucleation of new voids is also considered, and they named this new model Gurson-Tvergaard-Needleman (GTN). In both Gurson and GTN damage models, it is assumed that the matrix metal is isotropic and obeys the von Mises yield function. The GTN damage model, validated by

experimental results, has been used to investigate damage in various processes [11-13]. Khademi et al. [14] analyzed the stretch-bending process using the GTN damage model, and their analysis results agreed with experimental tests with reasonable accuracy. Using the GTN model, Sun et al. [15] accurately predicted the experimental forming limit diagrams (FLDs) of the AZ31 sheet, which were in good agreement with reality. In their research, Kami et al. [4] applied the anisotropic GTN model to the square deep drawing process of AA6016. Banabic and Kami [16] also implemented the anisotropic GTN model to investigate the role of voids in the matrix material of sheet metal.

In damage mechanics models based on finite element solutions, when the material enters the softening zone, changing the mesh size affects the accuracy of the analysis results. This problem is more apparent in porous materials because increasing porosity leads to softening [17]. Santos et al. [18] analyzed the behavior of advanced high-strength steels (AHSS) based on the GTN model using uniaxial tensile data and initial microvoids.

Porous metal plasticity is based on Gurson's porous metal plasticity theory. In the original formulation of the Gurson model, only the growth of pre-existing voids is considered. In other words, this model does not consider the creation of voids while inducing strain on the material. While the GTN damage model considers the creation of voids, the results obtained from this method are more accurate and closer to reality.

In this paper, the drawing depth of the St12 sheet in the square deep drawing process is obtained using numerical analysis with the GTN damage model and the porous metal plasticity model. The results obtained from the two models are examined and compared. Abaqus software was used to analyze the process numerically. GTN damage model has been implemented into the Abaqus software by writing a UMAT subroutine. Another numerical analysis was done using the porous metal plasticity model available in Abaqus software, and the results of these two analyses were compared.

2 DAMAGE MODELS

2.1. GTN Damage Model

Many of the damages in structures, metal, and non-metal parts, etc., are due to defects such as poor design, defects in the structure of engineering materials, and insufficient attention to phenomena such as fatigue, corrosion, etc. Extensive research has been done to identify the causes of these problems and prevent their occurrence, which is the starting point of failure mechanics. This research examines how the cracks are created and grown. The analysis of damage caused to materials is done with several models. One of the models presented based on

the combination of plasticity and damage, is the Gurson model [7], which describes the behavior of porous materials. Then, the Gurson model was modified by Tvergaard and Needleman and presented as the Gurson-Tvergaard-Needleman (GTN) model. This model is considered to describe the behavior of ductile porous materials in ductile failure. According to the GTN model, the ductile failure of the material is divided into three stages [19]. The first stage is the nucleation of the voids, the second stage is the growth of the voids, and the third stage is the coalescence of micro-cracks, while the Gurson model considers only the first stage (nucleation of voids).

According to the GTN damage model, ductile failure occurs in the following three stages:

1. The nucleation of voids is due to the separation of particle breakage, the contact surface between the matrix material and particles, or micro-cracks of the matrix material.
2. The growth of voids leads to the growth of the existing voids.
3. The coalescence of micro-cracks is caused by voids when the void volume fraction (VVF) reaches the final value, which leads to a decrease in the load-bearing capacity of the material.

Because the Gurson model, unlike the triaxial stress state, for low-stress triaxialities greatly exaggerated the failure strains, Tvergaard et al. [20] rewrote the model as follows by adding three parameters q_1 , q_2 , and q_3 to the Gurson model:

$$\Phi = \frac{\sigma_{eq}^2}{\sigma_y} + 2q_1 f \cosh \left[\frac{3}{2} q_2 \frac{\sigma_m}{\sigma_y} \right] - (1 + q_3 f^2) = 0 \quad (1)$$

Where Φ , σ_{eq} , σ_y , σ_m and f are yielding potential, Von-Mises equivalent stress, matrix yield strength, hydrostatic stress, and porosity, respectively.

To take into account the fast softening of the material during the coalescence of voids, Tvergaard and Needleman [20-22] added the function $f^*(f)$ to the model (1), and the new yield function is called Gurson-Tvergaard-Needleman (GTN) as follows:

$$\Phi = \frac{\sigma_{eq}^2}{\bar{\sigma}^2} + 2q_1 f^* \cosh \left[\frac{3}{2} q_2 \frac{\sigma_m}{\bar{\sigma}} \right] - (1 + q_1^2 f^{*2}) = 0 \quad (2)$$

$\bar{\sigma}$ is the equivalent tensile flow stress, indicating the matrix material's microscopic stress-state [20]. f^* is the modified porosity, which is calculated as follows:

$$f^*(f) = \begin{cases} f & \text{if } f < f_c \\ f_c + \delta(f - f_c) & \text{if } f_c < f < f_F \\ f_U^* & \text{if } f > f_F \end{cases} \quad (3)$$

Where δ represents the acceleration of coalescence and is equal to:

$$\delta = \frac{f_U^* - f_c}{f_F - f_c} \quad (4)$$

Where f_U^* is ultimo value (is reached when the macroscopic fracture occurs) and is obtained as $f_U^* = \frac{1}{q_1}$ when $q_3 = q_1^2 \cdot f_c$ is the critical porosity corresponding to the beginning of the coalescence, and f_F is the porosity corresponding to the final fracture of the material.

The porosity evolution is due to void growth and void nucleation, so:

$$\dot{f} = \dot{f}_{growth} + \dot{f}_{nucleation} \quad (5)$$

Assuming matrix incompressibility:

$$\dot{f}_{growth} = (1 - f) \dot{\varepsilon}_{kk}^P \quad (6)$$

Where $\dot{\varepsilon}_{kk}^P$ is the trace of the macroscopic strain rates tensor.

$\dot{f}_{nucleation}$ is the contribution of the nucleation for the cases in which the plastic strain controls the nucleation:

$$\dot{f}_{nucleation} = A \dot{\bar{\varepsilon}}^P \quad (7)$$

Where $\bar{\varepsilon}^P$ is the equivalent plastic strain.

Chu and Needleman [23] proposed the normal distribution of void nucleation as follows:

$$A = \frac{f_N}{S_N \sqrt{2\pi}} \exp \left[-\frac{1}{2} \left(\frac{\bar{\varepsilon}^P - \varepsilon_N}{S_N} \right)^2 \right] \quad (8)$$

Where ε_N is the mean strain and S_N is the standard deviation.

GTN damage model has nine parameters that can be classified into three categories [19]:

Constitutive parameters: q_1 , q_2 , and q_3 . These parameters are commonly fixed.

Nucleation parameters: ε_N , S_N , and f_N . The values of ε_N and S_N are usually considered to be 0.3 and 0.1 for most materials, respectively. f_N is the volume fraction of particles available for void nucleation. In contrast, the initial void volume fraction (VVF) parameter f_0 concerns all the inclusions [24-25].

Porosity parameters: f_0 , f_c , and f_F . These three parameters are considered as material parameters. The

initial VVF parameter f_0 indicates the initial state of the material obtained by microscopic analysis of the undamaged material. The critical void volume fraction f_c is the volume fraction of voids that when the porosity of the specimen reaches this value, the rigidity of the specimen drops suddenly. There are several methods to determine f_c , but it is complicated. Sun et al. [26-28] stated that f_c can be obtained by fitting the numerical curve with the experimental one. The final void volume fraction f_f indicates the state of the material at the fracture phase. This parameter has a constant value, its value for each material can be obtained experimentally [29] and is considered an unimportant parameter [30].

2.2. The Porous Metal Plasticity Model

The porous metal plasticity model models materials behavior with a dilute concentration of voids with a relative density greater than 0.9. This model is based on Gurson's porous metal plasticity theory (Gurson, 1977) with void nucleation and, in BAQUS/Explicit, a failure definition defines the inelastic flow of the porous metal based on a potential function that characterizes the porosity in terms of a single state variable, the relative density.

3 NUMERICAL SIMULATION OF DEEP DRAWING PROCESS

ABAQUS/CAE standard/FEM commercial software was used to determine the maximum drawing depth in the square deep drawing process of the St12 steel sheet. The geometrical model for numerical simulation of the process is shown in "Fig. 1". The punch, die, and blank holder were modeled as rigid parts, while the metal sheet was modeled as deformable bodies with 4-node shell elements (S4R). The die was constrained in all degrees of freedom. The punch and the blank holder were fixed about all rotations and restricted to only moving downwards in the vertical direction along the y-axis. A friction coefficient of 0.1 was considered between all faces of the die and the sheet.

The fracture limits were determined based on the GTN damage model (by writing the UMAT subroutine) and the porous metal plasticity model.

Mechanical properties of St12 blanks obtained by standard uniaxial tensile test (ASTM E8/E8M) are given in "Table 1".

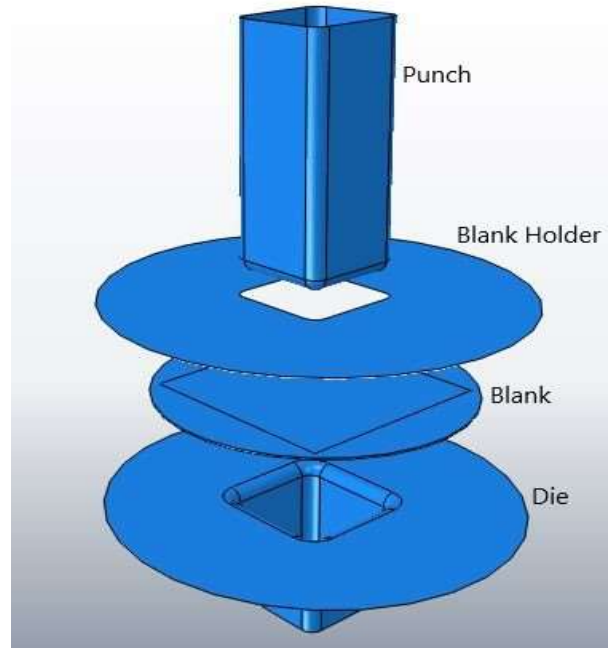


Fig. 1 Geometrical model of the deep drawing process in Abaqus software.

Table 1 Mechanical properties of St12

Variables (Unit)	Values
Thickness, t (mm)	0.7
Young's modulus, E (GPa)	210
Poisson's ratio, ν	0.3
Density ($\frac{Kg}{m^3}$)	7850
Strength coefficient, K (MPa)	510
Strain hardening exponent, n	0.21
Strain rate sensitivity exponent, m	0.006

3.1. Determining the Maximum Drawing Depth Using Gtn Damage Model

As mentioned, the GTN damage model (implemented to ABAQUS by writing UMAT subroutine) and the porous metal plasticity damage model (available in the ABAQUS software) have been used to determine the maximum drawing depth in the deep drawing process. The parameters of the GTN damage model should be determined correctly, usually by comparing experimental data and numerical results [19]. Since the determination of these parameters requires a lot of experimental data [19], [31-33] and may not lead to unique results [34-35], the values suggested by Tvergaard/Needleman are usually used for q_1 , q_2 , and q_3 . Values of these parameters are listed in "Table 2" [4].

Table 2 Values of GTN model parameters suggested by Needleman/Tvergaard [4]

Parameter	q_1	q_2	q_3 (q_1^2)	ε_N	S_N
Value	1.5	1	2.25	0.6	0.175

In the GTN model, the nucleation void volume fraction (f_N) and Critical void volume fraction (f_C) parameters play decisive roles in the ductile fracture of the material. In this paper, the values of parameters f_0 , f_N and f_F for carbon steel St12 sheet are taken from other research [36]. The value of the parameter f_C is considered to be 0.1 [37] (“Table 3”).

Table 3 Values of GTN model parameters for St12 [36-37]

Parameter	f_0	f_N	f_F	f_C
Value	0.00005	0.1	0.01	0.005

3.2. Determining the Maximum Drawing Depth Using Porous Metal Plasticity Damage Model

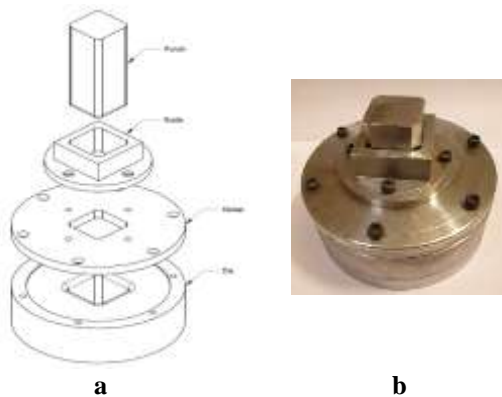
To determine the maximum drawing depth based on the porous metal plasticity model, values of the model parameters are considered as given in “Table 4”.

Table 4 Values of porous metal plasticity damage model parameters for St12

Parameter	q_1	q_2	q_3	f_F
Value	1.5	1	2.25	0.01
Parameter	f_C	ε_N	S_N	f_0
Value	0.005	0.6	0.175	0.00005

4 EXPERIMENTAL PROCEDURES

In experimental work, a deep drawing die assembly for square cross-section cups consisting of die, punch, blank holder, spacer, and punch guide, as shown in “Fig. 2”, was designed and made.

**Fig. 2** Designed die: (a): Parts of the die and, (b): Die assembly.

Experimental tests were performed using the SANTAM universal testing machine, STM 150 model (150 KN capacity). The experimental setup is shown in “Fig. 3”.

**Fig. 3** Experimental setup.

The 120 mm diameter circular blanks made of a 0.7 mm-thickness sheet of carbon steel St12 were used for experimental tests. The chemical composition of this material is given in “Table 5”.

Table 5 Chemical composition of St12

Material	Mn	C	Al	Ni	Cu
St12	0.21	0.049	0.029	0.024	0.017
Material	Cr	P	S	N	Si
St12	0.016	0.008	0.008	0.003	0.002
Material	Ti	B	Fe		
St12	0.001	2×10^{-4}	Bal.		

Mechanical properties of St12 blanks are obtained by standard uniaxial tensile test (ASTM E8/E8M).

5 RESULTS AND DISCUSSION

Figure 4 shows the drawn blank at the moment of fracture in experimental tests, the numerical simulation done by ABAQUS software using the GTN model, and the Porous metal plasticity model.

**a**



Fig. 4 Comparison of the blank at the moment of failure: (a): Experimental test, (b): Based on GTN damage model, and (c): Based on Porous metal plasticity model

The strain distribution in the sheet at the moment of sheet fracture was investigated to compare the two models. For this purpose, a path on the sheet was defined from the center of the sheet to near the outer edge of the sheet at the moment of fracture, then the strain distribution in the sheet on this path was determined based on both GTN and porous metal plasticity models. The defined path is shown in “Fig. 5”.

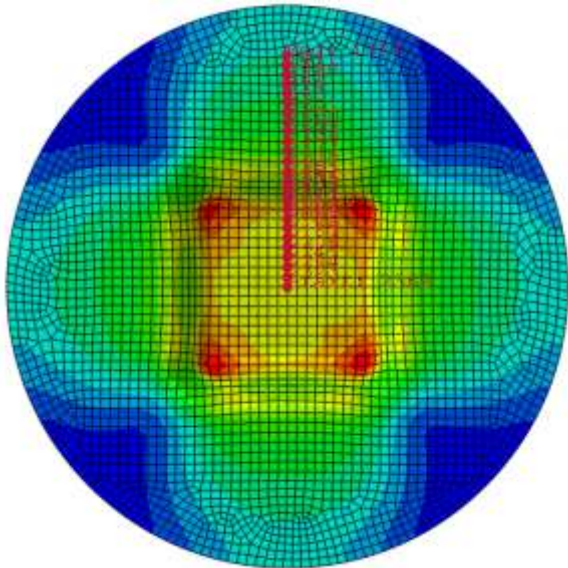


Fig. 5 The path defined to investigate the strain distribution at the moment of fracture.

Figure 6 shows the strain distribution of the specified path at the moment of sheet fracture for GTN and porous metal plasticity models. As it is evident in this figure, the stress value obtained based on the GTN damage model on this path is lower than the results of the porous metal plasticity model, which is closer to reality because, unlike the porous metal plasticity model, the GTN damage model considers the coalescence of micro-cracks.

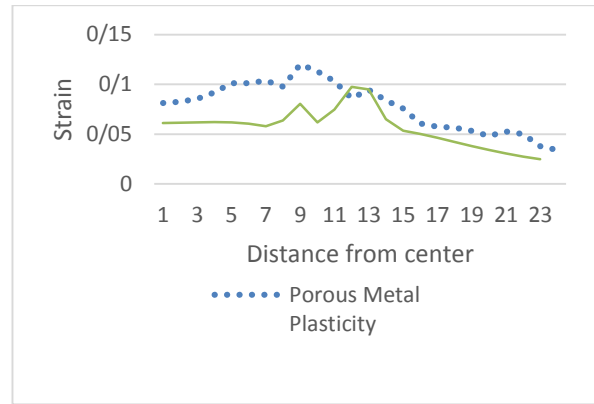


Fig. 6 Comparison of the strain distribution in the sheet at the moment of fracture based on the GTN and Porous Metal Plasticity models on the considered path.

In another comparison, the strain distribution at the moment of sheet fracture was investigated. For this purpose, an element on the drawn sheet wall was selected at the moment of fracture. Then, the strain distribution in the sheet on this element was determined based on GTN and porous metal plasticity models. The selected element is shown in “Fig. 7”. The reason for choosing this element is that it is located on the wall of the cup, which is under tension, and strain changes in this area occur relatively quickly.

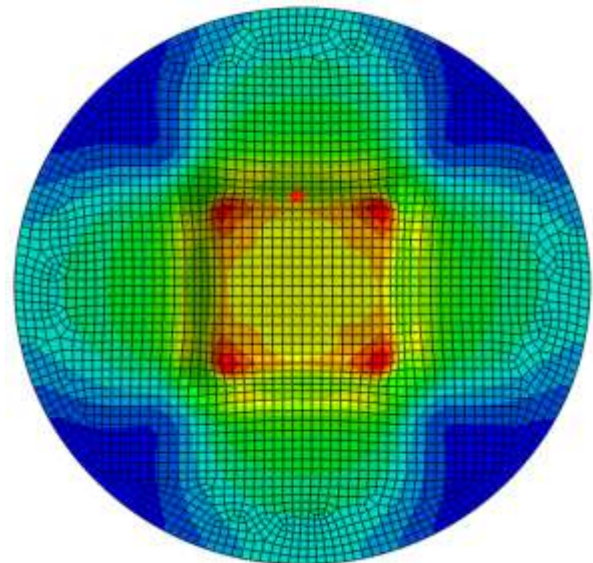


Fig. 7 The element considered to check the strain changes at the moment of sheet fracture.

In “Fig. 8”, the strain changes in the desired element at the moment of the sheet fracture are compared based on two damage models. Examining the strain changes in this element makes it possible to obtain the moment when the strain suddenly increases, which is when the fracture occurs.

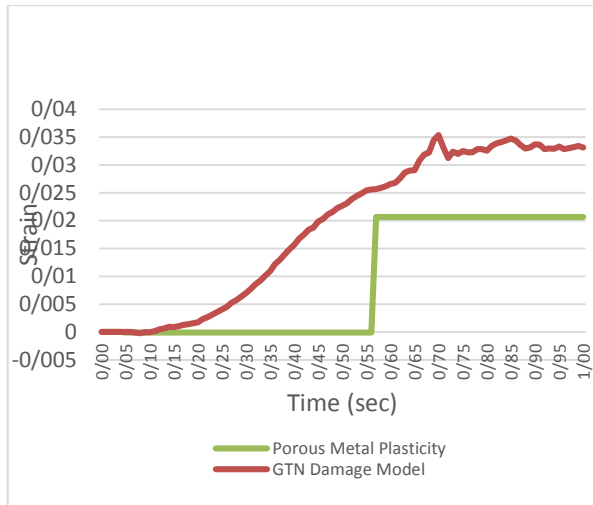


Fig. 8 Strain distribution on the considered element based on the GTN model and Porous Metal Plasticity.

Table 6 compares the fracture depth in numerical simulations based on the GTN damage model and porous metal plasticity model with the experimental one. As evident in this table, the results obtained from the GTN damage model are closer to the experimental results than the results of the Porous metal plasticity model, because, in the Porous model, the coalescence of micro-cracks is not considered.

Table 6 Depth of sheet fracture based on GTN damage model, Porous metal plasticity, and experimental test

Depth of fracture		
GTN (mm)	Porous metal plasticity (mm)	Experimental test (mm)
8.7	8.55	8.8

Figure 9 shows the effect of the friction coefficient between sheet metal, punch, and die on the maximum drawing depth for GTN and the porous metal plasticity models. As expected, by increasing the friction coefficient between the sheet and the punch and the matrix, the sheet fracture should happen earlier (the drawing depth decreases), which, as is evident in this figure, the GTN model has a better match than the porous metal plasticity model in this regard. The reason for this is that the results of the GTN damage model are more accurate due to the consideration of the coalescence of micro-cracks, unlike the porous metal plasticity model.

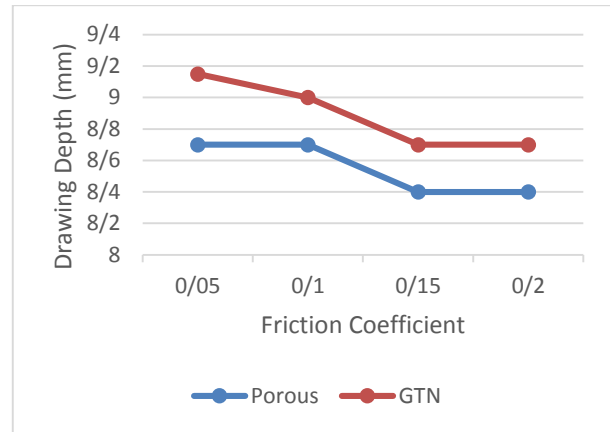


Fig. 9 Comparing the drawing depth obtained from the analysis based on the GTN model and the porous metal plasticity model in different friction coefficients.

The effect of the punch velocity on the maximum drawing depth in numerical simulations based on GTN and porous metal plasticity models is represented in “Fig. 10”. As it is evident in this figure, by increasing the speed of the punch, or in other words, by increasing the drawing speed, the sheet fracture happens sooner (the drawing depth decreases).

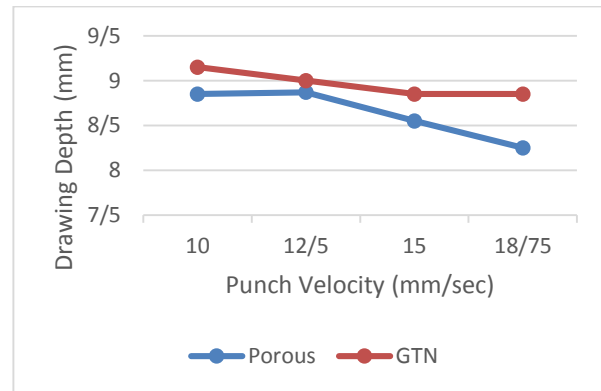


Fig. 10 Comparison of the drawing depth obtained from the analysis based on the GTN damage model and the porous metal plasticity model at different punch velocities.

Li et al.'s research was reviewed to verify the analyses' results. They analyzed the incremental sheet forming process based on the GTN damage model and the Hill 48 yield criterion by writing VUMAT in ABAQUS software. They compared the analyses' results with the results of experimental tests and observed that the GTN model's results were in good agreement with the test results [38].

6 CONCLUSIONS

In this paper, the deep drawing process was modeled in ABAQUS/Standard finite element software, and the

process analysis was done based on the GTN damage model and porous metal plasticity model. Next, to verify the numerical results obtained from the analysis, these results were compared with those obtained from the experimental tests, and the following results were obtained from this comparison:

- Both model results are in good agreement with the results of the tests.

- By comparing the drawing depth obtained from the GTN damage model and porous metal plasticity model to the result of experimental tests, it is found that the GTN damage model results are more consistent with the experimental tests.

- By examining how the drawing depth changes by changing the friction coefficient between the sheet and the die, it is concluded that the GTN damage model better analyzes the behavior of the sheet during forming.

- The changes in the drawing depth in the deep drawing process were investigated by changing the speed of the punch movement, and again, the results of the GTN model are more consistent with reality than the porous metal plasticity model.

In short, it can be said that the GTN damage model has more capabilities than the porous metal plasticity model for the analysis of sheet behavior because, firstly, the porous metal plasticity model does not take into account the f_N parameter that is present in the GTN model. Secondly, in the subroutine written for the GTN model, the mechanical properties of the sheet can be defined more precisely and comprehensively, which results in better results from the analysis based on the GTN model.

REFERENCES

- [1] Hosford, W. F., Caddell, R. M., Metal Forming: Mechanics and Metallurgy, Cambridge University Press, 2011.
- [2] Lange, K., Handbook of Metal Forming, McGraw-Hill Book Company, 1985, pp. 1216.
- [3] Johnson, W., Mellor, P. B., Engineering Plasticity, John Willey & Sons: New York, 1983.
- [4] Kami, A., Dariani, B. M., Vanini, A. S., Comsa, D. S., and Banabic, D., Application of a GTN Damage Model to Predict the Fracture of Metallic Sheets Subjected to Deep-Drawing, Proceedings of the Romanian Academy, Series A, Vol. 15, 2014, pp. 300–309.
- [5] Chen, F. K., Lin, S. Y., A Formability Index for The Deep Drawing of Stainless-Steel Rectangular Cups, The International Journal of Advanced Manufacturing Technology, Vol. 34, No. 9, 2007, pp. 878-888.
- [6] Padmanabhan, R., Oliveira, M. C., Alves, J. L., and Menezes, L. F., Influence of Process Parameters on the Deep Drawing of Stainless Steel, Finite Elements in Analysis and Design, Vol. 43, No. 14, 2007, pp. 1062-1067.
- [7] Gurson, A. L., Continuum Theory of Ductile Rupture by Void Nucleation and Growth: Part I—Yield Criteria and Flow Rules for Porous Ductile Media, Journal of Engineering Materials and Technology, Vol. 99, No. 1, 1977, pp. 2–15.
- [8] Tvergaard, V., Influence of Voids on Shear Band Instabilities Under Plane Strain Conditions, International Journal of fracture, Vol. 17, No. 4, 1981, pp. 389-407.
- [9] Tvergaard, V., On Localization in Ductile Materials Containing Spherical Voids, International Journal of fracture, Vol. 18, No. 4, 1982, pp. 237-252.
- [10] Tvergaard, V., Needleman, A., Analysis of the Cup-Cone Fracture in A Round Tensile Bar, Acta Metallurgica, Vol. 32, No. 1, 1984, pp. 157-169.
- [11] Chen, Z., Dong, X., The GTN Damage Model Based on Hill'48 Anisotropic Yield Criterion and Its Application in Sheet Metal Forming, Computational Materials Science, Vol. 44, No. 3, 2009, pp. 1013-1021.
- [12] Brunet, M., Sabourin, F., and Mguil-Touchal, S., The Prediction of Necking and Failure in 3 D, Sheet Forming Analysis Using Damage Variable. Le Journal de Physique IV, Vol. 6, No. C6, 1996, pp. C6-473.
- [13] Brunet, M., Mguil, S., and Morestin, F., Analytical and experimental studies of necking in sheet metal forming processes. Journal of Materials Processing Technology, 80, 1998, pp. 40-46.
- [14] Khademi, M., Mirnia, M. J., and Naeini, H. M., Numerical Analysis of Ductile Fracture in Stretch Bending of AA6061-T6 Aluminum Alloy Sheet Using GTN Damage Model, International Journal of Solids and Structures, Vol. 301, 2024, pp. 112947.
- [15] Sun, X., Mo, X., Liu, Y., Shen, W., Li, C., Li, Y., and Xue, F., GTN Poroplastic Damage Model Construction and Forming Limit Prediction of Magnesium Alloy Based on BP-GA Neural Network, Materials Today Communications, Vol. 41, 2024, pp. 110295.
- [16] Banabic, D., and Kami, A., Applications of the Gurson's Model in Sheet Metal Forming, In MATEC Web of Conferences, EDP Sciences, Vol. 190, 2018, pp. 01002.
- [17] Aravas, N., Papadioti, I., A Non-Local Plasticity Model for Porous Metals with Deformation-Induced Anisotropy: Mathematical and Computational Issues, Journal of the Mechanics and Physics of Solids, Vol. 146, 2021, pp. 104190.
- [18] Santos, R. O., Moreira, L. P., Butuc, M. C., Vincze, G., and Pereira, A. B., Damage Analysis of Third-Generation Advanced High-Strength Steel Based on the Gurson–Tvergaard–Needleman (GTN) Model, Metals, Vol. 12, No. 2, 2022, pp. 214. <https://doi.org/10.3390/met12020214>.
- [19] Miloud, M. H., Zidane, I., and Mendas, M., Coupled Identification of The Hardening Behavior Laws and Gurson–Tvergaard–Needleman Damage Parameters-Validation on Tear Test of 12NiCr6 CT Specimen, Frattura ed Integrità Strutturale, Vol. 13, No. 49, 2019, pp. 630-642.
- [20] Tvergaard, V., Needleman, A., Analysis of the Cup-Cone Fracture in A Round Tensile Bar, Acta metallurgica, Vol. 32, No. 1, 1984, pp. 157-169.

- [21] Tvergaard, V., Influence of Voids on Shear Band Instabilities Under Plane Strain Conditions, *International Journal of fracture*, Vol. 17, No. 4, 1981, pp. 389-407.
- [22] Tvergaard, V., On Localization in Ductile Materials Containing Spherical Voids, *International Journal of Fracture*, Vol. 18, No. 4, 1982, pp. 237-252.
- [23] Chu, C., Needleman, A., Void Nucleation Effects in Biaxially Stretched Sheets, *Journal of Engineering Materials and Technology*, Vol. 102, 1980, pp. 249-56.
- [24] Miloud, M. H., Imad, A., Benseddiq, N., Bachir Bouiadjra, B., Bounif, A., and Serier, B., A Numerical Analysis of Relationship Between Ductility and Nucleation and Critical Void Volume Fraction Parameters of Gurson-Tvergaard-Needleman Model. *Proceedings of the Institution of Mechanical Engineers, Part C: Journal of Mechanical Engineering Science*, Vol. 227, No. 11, 2013, pp. 2634-2646.
- [25] Cox, T., Low, J. J., An Investigation of The Plastic Fracture of AISI4340 and 18Nickel-200 Grade Maraging Steels, *Metall Trans A*, Vol. 5, 1974, pp. 1457-1470.
- [26] Sun, D. Z., Siegele, D., Voss, B., and Schmitt, W., Application of Local Damage Models to The Numerical Analysis of Ductile Rupture, *Fatigue & Fracture of Engineering Materials & Structures*, Vol. 12, No. 3, 1989, pp. 201-212.
- [27] Sun, D. Z., Voss, B., and Schmitt, W., Numerical Prediction of Ductile Fracture Resistance Behaviour Based on Micromechanical Models, *Defect Assessment in Components-Fundamentals and Applications*, 1989, pp. 447-458.
- [28] Sun, D. Z., Kienzler, R., Voss, B., and Schmitt, W., Application of Micromechanical Models to The Prediction of Ductile Fracture, *Astm Special Technical Publication*, Vol. 1131, 1992, pp. 368-378.
- [29] Guillemer-Neel, C., Feaugas, X., and Clavel, M., Mechanical Behavior and Damage Kinetics in Nodular Cast Iron: Part I. Damage Mechanisms. *Metallurgical and Materials Transactions A*, Vol. 31, No. 12, 2000, pp. 3063-3074.
- [30] Zhang, Z. L., Thaulow, C., and Ødegård, J., A Complete Gurson Model Approach for Ductile Fracture, *Engineering Fracture Mechanics*, Vol. 67, No. 2, 2000, pp. 155-168.
- [31] Kuna, M., Springmann, M., Determination of Ductile Damage Parameters by Local Deformation Fields, In *Fracture of Nano and Engineering Materials and Structures*, Springer, Dordrecht, 2006, pp. 535-536.
- [32] Djouabi, M., Ati, A., and Manach, P. Y., Identification Strategy Influence of Elastoplastic Behavior Law Parameters on Gurson-Tvergaard-Needleman Damage Parameters: Application to DP980 Steel, *International Journal of Damage Mechanics*, Vol. 28, No. 3, 2019, pp. 427-454.
- [33] Hadj Miloud, M., *Modélisation De La Rupture Ductile De L'acier 12 NiCr6 Par Le Modèle Micromecanique De Gurson* (Doctoral dissertation, Université Mohamed Boudiaf des Sciences et de la Technologie-Mohamed Boudiaf d'Oran), 2017.
- [34] Li, Z. H., Bilby, B. A., and Howard, I. C., A study of the Internal Parameters of Ductile Damage Theory, *Fatigue & Fracture of Engineering Materials & Structures*, Vol. 17, No. 9, 1994, pp. 1075-1087.
- [35] Zhang, Z. L., A Sensitivity Analysis of Material Parameters for the Gurson Constitutive Model, *Fatigue & Fracture of Engineering Materials & Structures*, Vol. 19, No. 5, 1996, pp. 561-570.
- [36] Guzmán, C. F., Experimental and Numerical Characterization of Damage and Application to Incremental Forming, (A Thesis submitted to the University of Liège in Partial Fulfillment of the Requirements for The Degree of Docteur en Sciences de l'Ingénieur), 2015.
- [37] Parsa, M. H., Etehad, M., and Matin, P. H., Forming Limit Diagram Determination of Al 3105 Sheets and Al 3105/Polypropylene/Al 3105 Sandwich Sheets Using Numerical Calculations and Experimental Investigations. *Journal of Engineering Materials and Technology*, Vol. 135, No. 3, 2013.
- [38] Li, J., Li, S., Xie, Z., & Wang, W., Numerical Simulation of Incremental Sheet Forming Based on GTN Damage Model, *The International Journal of Advanced Manufacturing Technology*, Vol. 81, 2015, pp. 2053-2065.